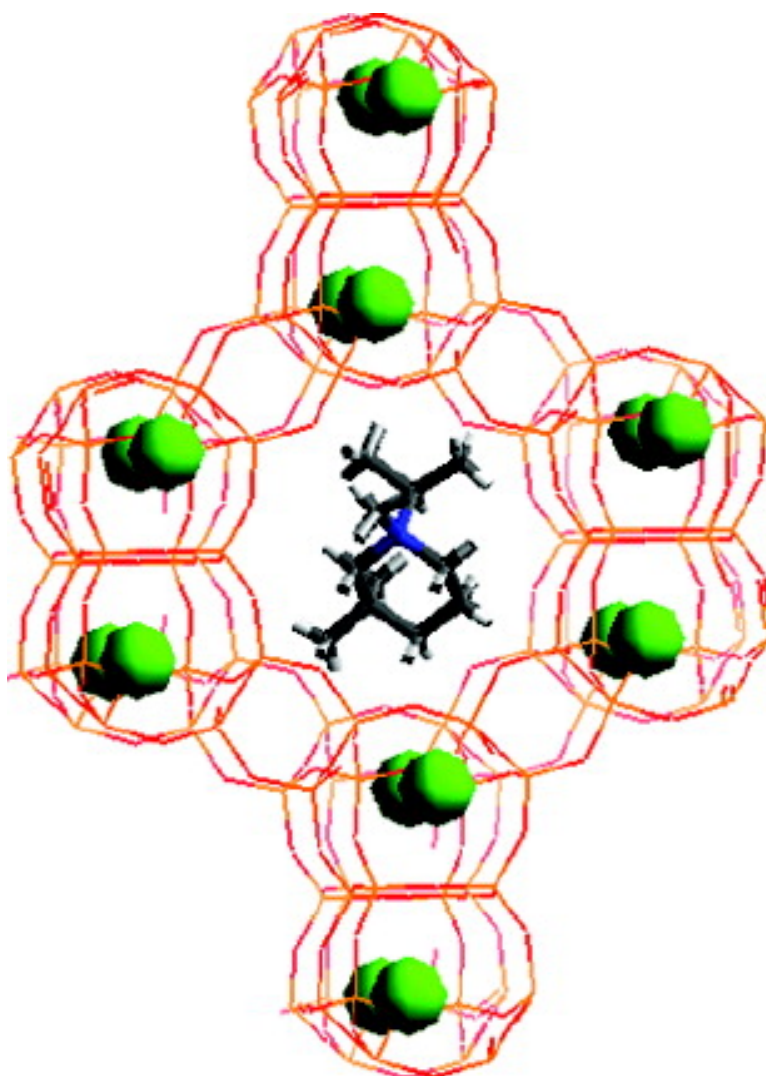Article

A Study of Piperidinium Structure-Directing Agents in the Synthesis of Silica Molecular Sieves under Fluoride-Based Conditions

Stacey I. Zones, Allen W. Burton, Greg S. Lee, and Marilyn M. Olmstead

More About This Article

Additional resources and features associated with this article are available within the HTML version:

- Supporting Information
- Links to the 3 articles that cite this article, as of the time of this article download
- Access to high resolution figures
- Links to articles and content related to this article
- Copyright permission to reproduce figures and/or text from this article

View the Full Text HTML

A Study of Piperidinium Structure-Directing Agents in the Synthesis of Silica Molecular Sieves under Fluoride-Based Conditions

Stacey I. Zones,*,[†] Allen W. Burton,[†] Greg S. Lee,[†,‡] and Marilyn M. Olmstead[§]

Contribution from the Chevron Energy Technology Company, Richmond, California 94802, and Department of Chemistry, University of California at Davis, Davis, California 95616

Received February 15, 2007; E-mail: sizo@chevron.com

Abstract: This study is a continuation of our efforts to understand the interplay in the self-assembly chemistry for formation of molecular sieves from guest organocations and inorganic silicon oxide. In this particular study we focus on the competitive interplay of the organocations and the synthesis cofactor fluoride anion. The anions play a key role in structure determination, as a function of net solution concentration. They compete with the role for the space-filling organocation in determining which molecular sieve host structure will be specified. In this study we look at this competition in the synthesis for a series of 33 different organocations derived from the piperidine ring system. Derivatives were prepared which both fixed substituents on the carbon and nitrogen centers on the ring. Results were discussed in terms of product selectivity from synthesis as a function of solution concentration for the reactants. A total of 17 different host topologies were found in this series, and a correlation was seen for (a) open-framework lattices (low framework densities) under the most concentrated reaction conditions and then (b) high framework density products once the conditions were more dilute. Some surprising synthesis differences are seen in comparing the performance of these structure directing agents (SDAs) in fluoride media vs hydroxide media (the more conventional environment for zeolite/molecular sieve syntheses involving silicate chemistry). Finally molecular modeling was used to understand some of the trends in product selectivity for closely related guest (SDA) candidates.

Introduction

In the past decade we have published several studies on zeolite synthesis in this journal. In those reports we have focused on the roles of structurally related organocations and how small changes in ring size or ring substituents affect the outcome of the crystallization of the inorganic hosts.[1-3] The goal has been to attain a sufficient understanding of this process, derived from a combination of experimental and computational approaches, that will lead us to a priori develop routes to prepare novel host inorganic structures. Each novel structure, once the organic guest has been removed (usually by thermal degradation) has the potential to provide new application advantages in areas such as catalysis and gas separations and in materials science applications for semiconductor components.[4]

The experiments in these previous studies were conducted under hydrothermal conditions in alkaline reaction media that provide conditions for "mineralization" of the silicate precursor reagents. The history of the zeolite synthesis field has largely been derived from a realization, over half a century ago, that natural zeolites form in hydrothermal reactions under slightly alkaline conditions found in certain geological contexts.[5] While pioneers in this synthesis effort modeled their early efforts around the inorganic, alkaline conditions that produced zeolites like **FAU**, **LTA**, and **LTL** (we will use the 3-letter codes for the zeolite structures, as given by the International Zeolite Association on their website www.iza.org, whenever they are available), the introduction of organocations led to a burgeoning of the number of zeolite structures discovered. Later it was recognized that fluoride anions, at near-neutral pH conditions, could function as a mineralizing agent to crystallize silica into zeolitic structures. The physical properties of these crystallization products were sometimes different from their analogues produced in hydroxide media. A significant distinction includes larger crystals containing fewer or no silanol defects within the lattice.[6,7] At the same time this synthesis route did not produce novel structures but instead made the same structure that the organic molecules might specify as structure-directing agents (SDA) under alkaline conditions.

[†] Chevron Energy Technology Co.
[‡] Current address: Lawrence Livermore Laboratory, Livermore, CA.
[§] University of California at Davis.
(1) Lee, G. S.; Nakagawa, Y.; Hwang, S-J.; Davis, M. E.; Wagner, P.; Beck, L.; Zones, S. I. *J. Am. Chem. Soc.* **2002**, *124*, 7024−34.
(2) Wagner, P.; Nakagawa, Y.; Lee, G. S.; Davis, M. E.; Elomari, S.; Medrud, R. C.; Zones, S. I. *J. Am. Chem. Soc.* **2000**, *122*, 263−273.
(3) Zones, S. I.; Nakagawa, Y.; Yuen, L-T.; Harris, T. V. *J. Am. Chem. Soc.* **1996**, *118*, 7558−7567.
(4) Wang, Z. B.; Yan, Y. *Adv. Mater.* **2001**, *13*, 1463.

(5) Barrer, R. M. *Zeolites and Clay Minerals as Sorbents and Molecular Sieves*; Academic: New York, 1978.
(6) Flanigen E. M.; Patton R. L. U.S. Patent 4 073 865, 1978.
(7) Guth, J.-L.; Kessler, H.; Caullet, P.; Hazm, J.; Merrouche, A. *Proc. Int. Zeolite Conf.* **1993**, *9*, 215.

Table 1. Concepts and Terms Used in the Study of Piperidinium Cations in Zeolite Sythesis

Piperidine derivatives: The following commercially available piperidines were functionalized at nitrogen to make a suite of organocation derivatives:
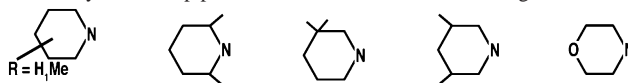
Framework density: This is defined as the number of silicon atoms, placed in tetrahedral sites, in the zeolite framework, placed in a given unit volume. We will typically refer to T (tetrahedral) atoms/1000 Å^3.

Zeolite product: This is the guest/host crystalline product which incorporates a piperidinium organocation into a silicate lattice. In this study there will also be some anionic fluoride (bonded to silica) found to be part of the structure.

SDA: This is short for structure-directing agent, used to describe the organocation in any given experiment.

Clathrasil: Clathrasils form with the SDA in the center of the cages or cavities, but the windows are too small for any transport of molecules in and/or out the cages. This is in contrast to molecular sieves which have pore systems which can be accessed.

Structure codes: The International Zeolite Association assigns three-letter structure codes for zeolites where the structure is known and agreed upon. The structure codes and details can be found at the website. Usually the codes have some relation to the published terminology. One of the best known zeolites is ZSM-5 (Zeolite Socony Mobil-5) and the code is derived from Mobil Five (MFI).

To facilitate our discussion in the Introduction and then onto the details of the study, here we have provided some helpful details. A number of the structures we will discuss have a graphical representation of their pore system in Appendix 1 (Supporting Information). More detailed views can be found in the IZA website. Table 1 defines and explains the key concepts used in our description of the important parameters we use and then product values we measure.

If we return to the developments in the use of fluoride anion syntheses, while the role of fluoride as "mineralizer" in these zeolite and molecular sieve synthesis reactions was recognized, the ability of this reaction type to generate novel crystallization products came later when Camblor and co-workers, working in the laboratories of Professor Corma at Valencia, Spain, began to greatly reduce the water contents in the reaction. The breakthrough came in the discovery that if reactions were carried out at low H$_2$O/SiO$_2$ ratios (i.e., 2−6) very open framework, all-silica molecular sieves could be produced. This was a first in this field of materials synthesis as the trend, heretofore, had been that all-silica products possessed high framework density, with low or no micropore volume. So, for example, a stellar product of this new approach was the synthesis of an all-silica **CHA** structure (low framework density and very high micropore volume).[8] As the reaction medium was diluted (higher H$_2$O/SiO$_2$ values), the **CHA** product gave way to products with higher framework densities.

Excited by this breakthrough, we recently performed a survey of synthesis with groups of organocations tested under these variable H$_2$O/SiO$_2$ conditions.[9] We also found it fascinating that the same trends in framework density of the host structures, which we had previously observed in alkaline conditions as a function of the extent of trivalent element substitution for silicate, emerged here as a function of the concentration of the silicate/SDA OH/HF reactants. When the amounts of these reagents remained constant but water content was varied, we were to learn that the role of fluoride was changing. The changes observed in the crystallization products were similar to the changes effected by the extent of lattice substitution (B or Al for Si) in alkaline conditions. The parallel is as follows (and is shown schematically in Figure 1): in this newer HF-based chemistry, we consider a reaction with SDA OH:SiO$_2$:HF of 0.5:1.0:0.5 in which the water content is systematically varied.

More open, lower framework density products form when water contents are low, and the higher density products of clathrasils and one-dimensional parallel pore systems (**MTW** being an example) emerge as dilution occurs in the reaction. We see the same trend for reactions in the conventional alkaline reaction in that the concentration of trivalent lattice-substituting reagent is the floating variable rather than the overall reaction concentration (how much water is used). As we discuss the details of our results, we will show the parallels in lattice structure types in terms of the subunits that specify the crystallization products. In this study we survey the effect of the reaction concentration in HF medium on a series of SDA built around the piperidine ring as the central building block of the charged SDA. We develop a number of SDA on the basis of the variation in the substituent placements on the ring and/or the charged nitrogen, and then we examine whether they or the overall reaction concentration (in effect the concentration of fluoride anion) control the guest/host product selectivity in the crystallization. Several interesting trends once again emerge which enhance our understanding about nucleation selectivity when multiple factors compete. We will also make observations of how framework density of products changes with reaction concentration within these series of experiments.

Experimental Section

Organocations (SDAs). A number of SDA's were synthesized by single or double alkylation steps to add substituents to the piperidine nitrogen. Table 1 shows a series of precursor amines, the building blocks we start with. Appendix 2 (Supporting Information) gives the synthesis examples that characterize the synthesis conditions for all the quaternary ammonium derivatives that we list in Table 2. Compounds were verified by NMR and by C, H, and N analyses.

Molecular Sieve Syntheses. The synthesis reactions were carried out in Parr 4745 stainless steel reactors that contain Teflon cups within. The 23 mL reactors were run at 43 rpm after loading onto spits within Blue M Convection ovens. This approach has been described in many of our previous studies.[10] Reactions were carried out at either 150 or 170 °C. Reaction steps generally followed a procedure of (a) combining 5 mmol of SDA OH and 10 mmol of Si(OEthyl)$_4$ in the Teflon cup, (b) letting the contents of the hydrolysis evaporate in a hood over several days (loss of ethanol and water), (c) readjusting the H$_2$O/SiO$_2$ to the desired ratio, and then (d) adding 50% HF (5 mmol) to form a thick gel. H$_2$O/SiO$_2$ values were adjusted to 3.5, 7.0, and 14.0 for each SDA studied. We had used these values in a previous study for examining changes in phase selectivity.[11]

(8) Camblor, M. A.; Villaescusa, L. A.; Diaz-Cabana M. J. *Top. Catal.* **1999**, *9*, 59.

(9) Zones, S. I.; Hwang, S-J.; Elomari, S.; Ogino, I.; Davis, M. E.; Burton, A. W. *Compt. Rend. Chim.* **2005**, *8*, 267−282.

(10) Zones, S. I.; van Nordstrand. R. A. *Zeolites* **1988**, *8*, 166.

(11) Zones, S. I.; Darton, R. J.; Morris, R. E.; Hwang S-J. *J. Phys Chem. B* **2005**, *109* 652

Figure 1. Generalized view of product formation in high silica zeolite synthesis. X_2O_3 refers to trivalent lattice substituents for silicon.

After the reactions were initially run 6−9 days, they were cooled and a sample was removed for scanning electron microscopy (SEM) observation of crystallinity. If no crystals were observed in the SEM, then the reaction was heated another 5−6 days and then the same process repeated. Once the field of the sample showed almost all crystals, the reaction contents were washed under filtration. After air-drying the reaction product was analyzed by X-ray diffraction to determine the phases present.

Characterization. The various samples taken for SEM analysis were diluted in 10−15 mL of water in vials. Then a sample of settled solid was collected for mounting into the instrument. The scanning electron micrographs were obtained using a JEOL JSM-6700F instrument. Powder X-ray diffraction analyses were carried out on a Siemens D-500 instrument. A single-crystal determination (for one of our products with suitably large crystals) was carried out on a Bruker ApexII instrument at the Department of Chemistry, University of California, Davis, CA, as has been previously described in some of our work.[12] In some instances elemental analyses were obtained on the guest/host products that had crystallized. These analyses were carried out by ICP methods, after acid digestion or fusion sample preparation, at Galbraith Analytical (Knoxville, TN).

Modeling Studies. These studies were carried out to examine the energy minimization prospects that might be associated with the formation of the guest/host complexes. We recently described a considerable body of comparison of experimental results with calculations for SDA stabilizations within cage-based zeolite structures.[13−17] Calculations were performed with the Cerius2[15] software using a combination of the Burchart[16] and Universal forcefields[17] to evaluate the van der Waals interactions of the SDA molecule with the zeolite framework and the intermolecular interactions of the SDA.

To simplify the calculations, we model each zeolite structure as an all-silica framework, and we neglect columbic interactions between the SDA molecule and the fluoride anions. In most cases the positions of fluoride anions are not precisely known. (Pulido et al. have recently described[18] a rigorous computational approach to determine the probable location of fluoride anions in as-made materials, but this is outside the scope of the current study.) Sastre et al. have performed calculations[19]

on all-silica frameworks prepared in fluoride media in which the fluoride anion was placed within the centers of double four-ring units in different framework structures. Their calculations showed that the noncolombic interactions between the SDA and the all-silica framework were 1 order of magnitude greater than the electrostatic contributions from the SDA−F^- interaction. In addition, the differences in the electrostatic terms of different SDA/framework pairs were usually negligible compared to the overall calculated energies. Short-range van der Waals forces, therefore, usually provide the dominant contributions to the stability of the SDA/framework composite.[20] However, we note that in a few instances the long-range interactions between the fluoride and SDA molecule may provide ample stabilization to alter the otherwise expected trends. For example, a study by Arranz et al. has recently demonstrated[21] how placements of fluorine in different positions of an SDA molecule may change the behavior of the SDA molecule by altering the electrostatic interactions between the SDA and the fluoride anions.

The calculations are performed on periodic structures using a single unit cell. No supercells are required for most of the cage-based frameworks considered since the molecular dimensions do not exceed the unit cell dimensions and since there are negligible interactions between SDA in neighboring cage structures (i.e., each cage effectively isolates its occluded SDA molecule). During the energy minimization process, the atoms of the zeolite framework are held fixed. To find the true global minimum for each SDA molecule, we exhaustively sample multiple initial configurations (and molecular conformations as appropriate). The stabilization we report is the difference between the energy of the molecule occluded in the framework and the minimum energy of the free (gas phase) molecule.

Since we are primarily concerned with how the silica phase is stabilized, we normalize the absolute stabilization energy (per mole of SDA) by dividing by the appropriate number of T atoms in the unit cell. For example, if there are four cages/unit cell, one SDA/cage (an assertion which is generally borne out by microanalytical data for the composition of the as-made products), and 88 T atoms/unit cell, the absolute energy/SDA is divided by 22 T atoms. Therefore, in general, we expect denser framework structures to have lower normalized stabilization energies when the absolute energies are approximately the same.

Results and Discussion

Products of the Runs Made. Our study continues our interest in the interplay between the H_2O/SiO_2 ratio in the fluoride synthesis and the type of molecular sieve that will form. The spatial features of the guest molecule (SDA) also have an influence on which actual product will nucleate and crystallize within a given reaction regime (extent of dilution, for example) Within these reaction regimes, Corma has stated that it is the concentration of the fluoride which is the key parameter.[22] We essentially achieve these changes by holding the reagent components fixed in absolute amounts and molar ratios (unto each other) and then allowing the quantity of solvent contribution, H_2O, to vary.

Concerning the SDA parameter as a contribution to phase selectivity, one can imagine building a host of SDA by changing the ring and nitrogen substituents on the piperidine ring. Our SDA synthesis centered on nitrogen alkylation, and in fact, a range of piperidine derivatives had been previously described by us, utilized in the alkaline, Al, and B synthesis reaction

(12) Zones, S. I.; Olmstead, M. M.; Santilli, D. S. *J. Am. Chem. Soc.* **1992**, *114*, 4195.
(13) Burton, A. W.; Lee, G. S.; Zones, S. I. *Microporous Mesoporous Mater.* **2006**, *90* (1−3), 129−144.
(14) Software is the Cerius2 V.2.1 product of BioSym and MSI Corp.
(15) Burchart, E. d. v. Studies on Zeolites: molecular mechanics, framework stability and crystal growth. Ph.D. Thesis, 1992.
(16) Rappe, A. K.; Casewit, C. J.; Colwell, K. S.; Goddard, W. A., III. *J. Am. Chem. Soc.* **1992**, *114*, 10024.
(17) Lewis, D. W.; Freeman, C. M.; Catlow, C. R. A. *J. Phys Chem.* **1995**, *99*, 11194−11202.
(18) Pulido, A.; Corma, A.; Sastre, G. *J. Phys. Chem. B* **2006**; ASAP article.
(19) Sastre, G.; Leiva, S.; Sabater, M. J.; Gimenez, I.; Rey, F.; Valencia, S.; Corma, A. *J. Phys. Chem. B* **2003**, *107*, 5432−5440.

(20) Sastre, G. Personal communication.
(21) Arranz, M.; Perez-Pariente, J.; Wright, P. A.; Slawin, A. M. Z.; Blasco, T.; Gomez-Hortiguela, L.; Cora, F. *Chem. Mater.* **2005**, *17* (17), 4374−4385.
(22) Corma, A. *Proc. Int. Zeolite Conf.* **2004**, *14*, 1.

Table 2. Zeolite Phases That Result from Use of Piperidine SDAs[a]

Clathrates Were Formed

Code	Structure	150° C/43RPM H₂O/SiO₂ 3.5	7.0	14.0	170° C/43RPM H₂O/SiO₂ 3.5	7.0	14.0
G11	(structure)	AST	NON>AST	NON	AST	AST>NON	NON
G74	(structure)	AST	Amo>AST	DDR			
G210	(structure)	NON	NON	Amo/NON			
G200	(structure)	NON	NON	NON			
G32	(structure)	BEA* A>B	BEA*	DDR		BEA* A>B	Unknown
G24	(structure)	MEL		MTW	MFI	MFI/MTW	MTW
G25	(structure)	NON	NON	NON			
G80	(structure)	BEA	DDR	DOH	SGT	DDR	DOH
G65	(structure)	MFI	DOH	DOH	MFI	DOH	DOH
G39	(structure)	STF	STF	STF	STF	STF	
G49	(structure)	MEL/MFI	MEL/MFI	MTW			
G55	(structure)		NON	NON	NON		

Clathrates No Longer Can Form

Code	Structure	150° C/43RPM H₂O/SiO₂ 3.5	7.0	14.0	170° C/43RPM H₂O/SiO₂ 3.5	7.0	14.0
G61	(structure)	MFI	MFI	MFI		STF?	
G201	(structure)	BEA*	MTW	MTW			
G40	(structure)	SFF	SFF	Amo>SFF	SFF	SFF	
G50	(structure)	MEL	MEL	MEL			

Clathrates No Longer Can Form

Code	Structure	150° C/43RPM H₂O/SiO₂ 3.5	7.0	14.0	170° C/43RPM H₂O/SiO₂ 3.5	7.0	14.0
G51	(structure)	STF	STF	NES	CON/STF	CON?	Amo
G71	(structure)	MFI	MFI	MFI			
G69	(structure)	BEA	NES/BEA	NES/Amo	CON	STF/CON	
G52	(structure)	MEL	MEL	MEL			
G122	(structure)	ITE	ITE	ITE/Amo			
G93	(structure, Bz)	EUO	EUO	EUO			
G123	(structure)	AST	ISV				
G212	(structure)	BEA*	BEA*	NON			
G213	(structure)	BEA*	BEA*	BEA*			
G211	(structure)	BEA	BEA	MTW			
G202	(structure)	BEA	odd BEA	MTW			
G77	(structure)	BEA/STF	STF	STF	MEL		STF
G81	(structure)	BEA	BEA		BEA	BEA	BEA
G86	(structure)	CON	CON	CON			
G73	(structure)	MEL	MEL	MEL			
G121	(structure)	BEA	BEA	Amo			
G97	(structure)	STT	STT	Unknown	Unknown	Unknown	Unknown

[a] 170° data in red for ease of identification.

systems.[23] Once we have considered the results obtained for this range of SDA operating in the HF medium as a function

(23) Nakagawa, Y.; Lee, G. S.; Harris, T. V.; Yuen, L-T.; Zones, S. I. *Microporous Mesoporous Mater.* **1998**, *22*, 69−85.

of reactant dilution, we will compare the products from the other type of zeolite synthesis reaction medium.

Table 2 lists our crystalline product results for the variation of 3 H₂O/SiO₂ ratios at 150 °C and 43 rpm. In some instances

(where there was sufficient SDA available) data are also given for 170 °C. Corma has discussed the changes in product selectivity with regard to temperature variation, describing how the energetics of nucleation might be influenced.[20] For that reason we were interested in exploring that issue as well. We do see some changes in the table in going from 150 to 170 °C, but more often our product selectivity remains unchanged.

1. Clathrate Formation. In a much earlier study, focused on product selectivity changes for all-silica clathrates as a function of temperature change, Gies also noted some changes in product selectivity. In these experiments where large amounts of amine were used as guest molecule and, in essence, cosolvent, for sealed tube hydrothermal reactions, Gies developed a view that the cage size of the possible clathrate product would follow certain rules via temperature of the reaction.[24] His findings are relevant for our work here, although we are using charged SDA, because as our SDA remain small and the reactions are diluted, there is a preponderance of clathrate formation (our study generates 5 different ones).

The table is organized in increasing size of the SDA tested in the reactions. The simplest, starting point derivative contains no ring substituents and only methyl groups on the nitrogen. This compound, G11, has C/N^+ of 7, and this will be the smallest SDA we consider. It remains a very successful guest molecule for Nonasil (**NON**), a clathrate material, over a range of synthesis ratios, although **AST** is seen in the more concentrated instances. The table contains progressively larger SDA with respect to either ring substitution or to the *N*-alkyl derivatives. A number of mono- and di-*N*-ethyl derivatives were made. There are a few unusual SDA's that do not really constitute a series, per se (and they will be discussed), and then we arrive at the largest derivatives, where spiro SDA's have been made. These are charged compounds where two rings are developed, in spiro fashion, around the tetrahedron centered on the quaternary nitrogen.

Two pronounced trends can be seen in the table. The smaller SDA lead to clathrate structures. Derivatives, whatever they might be, if they are small, will favor clathrates. The selectivity as to which clathrate may change as a function of dilution and temperature. The second trend is that there is generally a change in product selectivity over the dilution range and the highest framework density product is mostly found at the more dilute run conditions. Higher framework density ($TO_2/1000$ Å³) will translate into lower void volumes. The products we observe in this study are either clathrate products or a one-dimensional zeolite product, **MTW**. Appendix 1 shows a number of the structure representations for the 17 product topologies given in Table 2. We had often observed **BEA*** zeolite as the low-density framework product and then lattices like **MTW** as the high framework density candidates as we changed the net boron[25] or aluminum concentration in the syntheses.[26] In this study we will see that **BEA*** and **MTW** do represent the extreme boundary conditions for product framework densities. Figure 1 shows a representation of the bifurcation of open framework structures, typically richer in 4-ring subunits, and then the formation of the higher framework density clathrates like **NON** and one-dimensional pore products like **MTW**. Whether a

Table 3. Framework Densities of Materials

zeolite	DLS optimization	T/1000 Å³
BEA	15.3	15.1
MFI	18.4	17.9
MEL	17.4	17.6
STF	16.9	17.3
SFF	17.8	17.2
ITE	15.7	16.3
NES	16.4	17.7
EUO	17.1	18.2
SGT	17.5	17.8
NON	17.6	19.3
AST	15.8	17.8
DDR	17.9	17.6
DOH	17.0	18.5
MTW	18.2	19.4
CON	15.7	16.1
STT	17.0	17.0
ISV	15.4	15.0

clathrasil or a phase like **MTW** forms, at the extreme conditions of the two systems, depends largely on the size of the SDA.

2. Framework Densities. In Table 3 we show the framework densities for the 17 zeolite topologies our syntheses produce. We show values from two different types of measurements. It is important to appreciate the distinction between these two reported values. The T-atom density in the first column is obtained from a DLS refinement of the all-silica framework in its *highest possible framework symmetry*. The second column shows the actual T atom density determined by (crystallographic) experiment for the most siliceous composition reported for that framework type. Comparison of the two columns reveals that often there are significant inconsistencies between what Nature prefers and what is determined by the DLS optimization. In fact, many of the entries within the first column show trends that are counterintuitive. For example, frameworks that differ by a single symmetry operation (like a mirror plane or inversion center) should be expected to have similar framework densities. The pairs **STF/SFF** and **MFI/MEL** are two such examples. However, the DLS refinements for each pair show that the T atom densities differ by almost 1 T atom. The experimental T atom densities are actually very close. There are several examples where the T atom densities determined by DLS differ from the experiment by more than 1 T atom: **NES**, **EUO**, **NON**, **AST**, **DOH**, and **MTW**. Because the DLS optimization uses the highest possible symmetry for each framework, atoms are sometimes constrained to occupy high-symmetry positions that do not allow the structure to relax to a preferred symmetry of lower energy. Also, in some cases the structure may have atoms that are disordered about high-symmetry positions. Most of the frameworks cited above do indeed have several atoms that occupy high-symmetry positions. For example, the highest possible symmetry of **AST** is $Fm\bar{3}m$, whereas the true symmetry of the all-silica material is I4/m.[27] The high cubic symmetry demands T—O—T bond angles of 180°, whereas the lower tetragonal symmetry does not. The relaxation of the symmetry constraints in the cubic space group allows the framework to adopt a structure with more reasonable bond geometries. Similar arguments may be presented for the **NON** framework, which requires several 180° oxygen angles in its highest symmetry. We therefore believe the experimentally

(24) Gies, H.; Marler, B. *Zeolites* **1992**, *12*, 42—49.
(25) Zones, S. I. *Microporous Mater.* **1992**, *2*, 281—287.
(26) Zones, S. I.; Nakagawa, Y.; Lee, G. S.; Chen, C. Y.; Yuen, L-T. *Microporous Mesoporous Mater.* **1998**, *21*, 199—211.

(27) Caullet, P.; Guth, J. L.; Hazm, J.; Lamblin, J. M.; Gies, H. *Eur. J. Solid State Inorg. Chem.* **1991**, *28*, 345—361.

A R T I C L E S

determined entries in the second column provide a more reliable measure of the density.

3. Open-Framework Products (Lower Density). In this study we believe high concentrations of fluoride influence the propensity to form 4-ring subunits within the specified inorganic host silicate lattice. That the incorporation of higher populations of 4-rings would be related to more open-framework products is consistent with a study reported by Meier concerning the search for high void volume zeolites.[28] The goal of many synthesis efforts has been to make open-framework materials, and Meier has shown that the most desirable subunit is 3-rings. The 4-rings were also shown to be preferable over the 5-rings seen in many high framework density products and missing from very open structures such as **FAU**, **LTA**, and **CHA**. The attempt to derive such lattices containing 3-rings has led to the use of lattice components which favor this with rare examples of beryllium[29] and much greater effort in research using zinc to generate materials like VPI-7-10 from the Davis laboratory[30] and more recently some success for the efforts from Gies' group.[31] In recent years another breakthrough has come again from Corma's group where a number of new materials (with and without using the fluoride route) have been generated by using germanium in place of a minor amount of the silica. From crystallographic characterization of these germanosilicate products, it is clear that the Ge favors the formation double 4-rings in the lattices where it becomes incorporated.[32] The ability of germanium to form open-framework materials is exemplified by the recent discovery of ITQ-33, a germanosilicate with an $18 \times 10 \times 10$ pore system that possesses both double four-ring and three-ring subunits.[33]

4. Trends for Related SDA's. For the molecules we used as SDA in the syntheses, 17 different lattice topologies were encountered (they are also listed in Table 3). We did not find any products with previously unreported structures although G97 does make an unusual layered structure that we will discuss. In Table 3, the range of framework densities span a range of values from near 15 TO$_2$/1000 Å^3 for **BEA** and **ISV** to >19 for **MTW** and **NON**. From the 17 products obtained in the ensemble of experiments, we can make these observations: (a) β zeolite (**BEA***) is a frequent product for large enough SDA in experiments with low H$_2$O/SiO$_2$ conditions. However, surprisingly, there are a few SDA that seem small enough (C/N$^+$ = 9) to make clathrate products. G32, for example, makes an interesting version of **BEA*** as well (vide infra). (b) **NON** is frequent for the higher dilution end, unless the SDA is sufficiently large. (c) **MTW** becomes the more frequent, high-dilution product as the SDA either become too large to make **NON** or unable to fit into the cage of **NON** because of the shape of the molecule. (d) There remain certain SDA's which exhibit very high selectivity for certain host lattice structures and produce them over a range of concentration conditions.

While the smallest SDAs have good selectivities for **NON**, there are some interesting exceptions. We can see when C/N$^+$

= 7 or 8, that SDA's like G11, G200, and G210 all have abilities to help crystallize **NON**. But G74 and the one-carbon larger G32 (both with methyls next to the methyl-substituted nitrogen) do not. Is there a poor fit in **NON** for these candidates? On the other hand, C/N$^+$ = 9 (G25) and 10 (G55) both have good selectivities for **NON** and both have the 3,3-dimethyl ring feature. There may be an attractive fit for these derivatives that eventually is lost for the yet larger 3,3-dimethyl SDA's (G51, -69, -93, and -81). So conformational details on the SDA are just as important as overall size in determining the SDA role in product selectivity. Where the given methyl groups occur off the piperidine ring matters.

One of the structures formed by a few SDA's in high specificity is **MEL**. G50 has been the best SDA for **MEL** crystallizations in alkaline medium as shown by Nakagawa, Terasaki, and others.[34] We also find here that G50 specifies **MEL** over a range of concentrations and both temperatures considered. Here is a case where the phase selectivity of the SDA is not affected by the fluoride concentration. We had previously mentioned that this condition is relatively infrequent in the study of SDA and changing fluoride concentrations (a glance at Table 2 supports this view).[12] Interestingly, there are some SDA's in the table that have some of the features of G50 and they produce **MEL** in some but not all reaction conditions. The key detail in the piperidine derivatives that do show some selectivity for **MEL** is the positioning of methyl groups at ring positions 3 and 5. This can be seen in derivatives G52, G73, and G24. The importance of the two methyl groups at the 3 and 5 positions of the ring has previously been highlighted in calculations for the SDA fit in **MEL** carried out by the group of von Koningsveld.[35] There they explain why this SDA is selective for **MEL** rather than the closely related **MFI**.

If the methyl groups are now in the 2,6 positions relative to nitrogen at position 1, then the more likely products are **STF** and **SFF** from SDA G39 and 40. These two host structures are related by a single symmetry operation change involving an inversion center or mirror plane as previously described.[36] A third SDA with the same placement of substituent methyls, G77, also yields **STF** in some reactions. However, it is interesting that the G97, one methylene unit larger, will not make the **STF** but rather leads to either an unknown layered material or to an **STT** product, which possesses the novel 9- by 7-ring channel system.

At first glance, it may appear that arguments based upon space-filling do not adequately rationalize some of the cases of specificity we present. There is one morpholine derivative in the table, G71. It has a methylene in the ring (position 4) replaced by oxygen. There are the methyl groups at positions 3 and 5 as we saw in the **MEL**-specific SDA. The change in CH$_2$ to O might not be expected to manifest dramatic differences in space-filling, but modeling work discussed below shows that the change is sufficient to influence product selectivity. The SDA with oxygen now does not make **MEL** but instead produces the closely related **MFI** in each synthesis concentration.

(28) Brunner, G. O.; Meier, W. M. *Nature* **1989**, *337*, 146−147.
(29) Cheetham, A.; Fjellvag, H.; Gier, T. E.; Kongshaug, K. O.; Lillerud, K. P.; Stucky, G. D. *Stud. Surf. Sci. Catal.* **2001**, *63* (135), 788−795.
(30) Annen, M. J.; Davis, M. E. *Microporous Mater.* **1993**, *1*, 1.
(31) Rohrig, C.; Gies, H. *Angew. Chem., Int. Ed.* **1995**, *34*, 63−65.
(32) Sastre, G.; Vidal-Moya, J. A.; Blasco, T.; Ruis, J.; Lorda, J. L.; Navarro, M. T.; Rey, F.; Corma, A. *Angew. Chem., Int. Ed.* **2002**, *41*, 4722−26.
(33) Corma, A.; Diaz-Cabanas, M. J.; Jorda, J. L.; Martinez, C.; Moliner, M. *Nature* **2006** *443*, 842−845.

(34) Ohsuna, T.; Terasaki, O.; Nakagawa, Y.; Zones, S. I.; Hiraga, K. *J. Phys. Chem. B* **1997**, *101*, 9881−85.
(35) Njo, S. L.; Koegler, J. H.; von Koningsveld, H.; van De Graaf, B. *Microporous Mater.* **1997**, *8*, 223.
(36) Wagner, P.; Zones, S. I.; Medrud, R. C.; Davis, M. E. *Angew. Chem., Int. Ed.* **1999**, *38*, 1269.
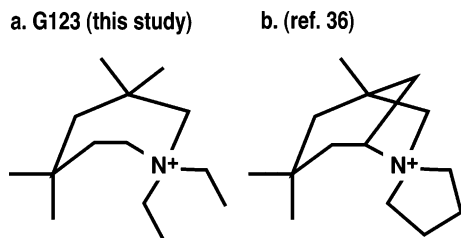
a. G123 (this study)   b. (ref. 36)

Figure 2. Two surprisingly similar SDA molecules (root ring systems different) in possible conformations leading to **ISV**.

Unique product selectivity can also be rationalized for the single SDAs in the table that give strong preference to forming **ITE** and **EUO** (G122 and -93, respectively). Previously we had seen that **ITE** was very much favored by polymethylation of the rings in either piperidine or bicyclic SDA systems. These results were obtained in alkaline reaction conditions, and reactions with boron seemed particularly predisposed to form **ITE** for a range of these types of SDA's.[37] Burton et al. recently showed that for a series of cage-based host lattices the favorable SDA's for making these products show good van der Waals stabilization in the cages.[14] The polymethylated rings provide a nearly maximized surface for the SDA to present methyl protons to the host silicate lattice surface within the cage. Particularly for the smaller SDA candidates which succeed in producing borosilicate **ITE/RTH** phases, the tendency of the borosilicate reaction to be more successful in producing this lattice host than either all-silica or aluminosilicate reaction mixtures may be related to the solubility and mobility of borate ions in the reaction mixture. This may be an important feature of the successful nucleation of this lattice.[38] We will show toward the end of the discussion that some of the SDA's that produce **ITE** under borosilicate conditions fail to do so here in the all-silica HF reaction system. But the polymethylated homopiperidine G122 is especially effective in producing **ITE** products. For this seven-member ring there are 6 methyl substituents and **ITE** is the only product it makes.

If G123 is used, which is built from the homopiperidine with 4 ring methyls, but the N-substituents are now ethyl groups (were methyl in G122), the structure **ISV** forms. This material, recently reported by Corma and co-workers,[39] has a structural relationship to **BEA*** but also contains double 4-rings, and it is not surprising that a rather large SDA templates it. We were initially surprised by this result, but a comparison of the SDA structures G123 and the [3.2.1]azaoctane derivative used by Corma[40] reveals surprisingly similar features even though their synthesis routes are so different. See Figure 2 for the comparison.

SDA Size (C/N$^+$) and the Concentration Effect. We have been stating that the final product obtained in these guest/host complexes is a result of both the SDA and the net concentration of the reaction. While the previous section covered the selectivities of classes of SDA, based upon their structural details, here we note some trends built around the size of the molecules alone.

(37) Nakagawa, Y. U.S. Patent 5 268 161, 1993, and refs 2 and 23 herein.
(38) Zones, S. I.; Hwang, S-J. *Microporous Mesoporous Mater.* **2003**, *58*, 263–27.
(39) Corma, A.; Diaz-Cabanas, M. J.; Fornes, V. *Angew. Chem., Int. Ed.* **2000**, *39*, 2346–49.
(40) (a) Sastre, G.; Cantin, A.; Diaz-Cabanas, M. J.; Corma, A. *Chem. Mater.* **2005**, *17* (3), 545–552. (b) Villaescusa, L. A.; Barrett, P. A.; Camblor, M. A. *Angew. Chem., Int Ed.* **1999**, *38*, 1997.
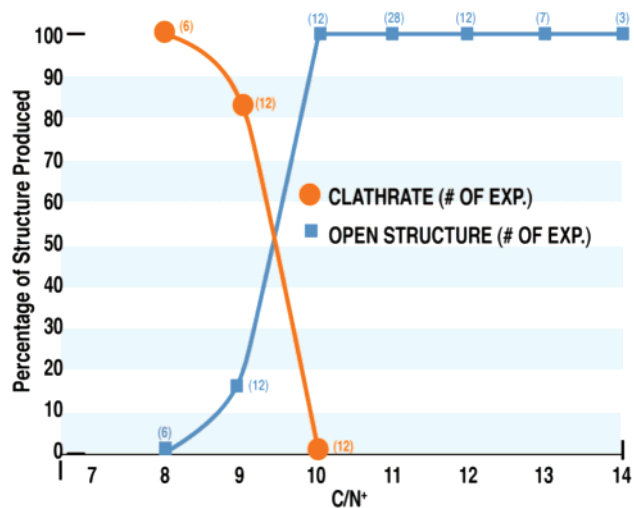
Figure 3. Clathrate versus open framework formation. Numbers in parentheses indicate how many results contribute to this graph point.

Figure 3 shows the relative production of clathrate structures vs open-framework products for all reactions considered. One can see a very sharp change in the product type as the molecules reach a size of 8 or 9 carbons and a single N$^+$. All molecules we considered in this study had only a single charged nitrogen.

If a clathrate cannot be made (cages are no longer large enough) as the C/N$^+$ increases, then what is the fate of the product in the regime (high dilution) where high framework density clathrates are favored? If the molecule possesses a long axis, then **MTW** is often the default structure. In our previous study for classes of compounds which could not fit in **MTW**, we had seen that the most dilute conditions would sometimes produce what we could consider a "cage-based" host structure, but the cages were sufficiently large and interconnected that there were also usable channels systems in the product. Clathrates are generally described as having no usable channels. In the case of these next series of molecules that are too large to form traditional clathrates at the high-dilution experiment, products with 10-ring portals, **STF**, **SFF**, and **NES**, are seen, and in one instance, we see **STT** (9 and 7 rings!).[41]

Even if there is an important space-filling preference in terms of what guest/host complexes can form, once there is more than one viable possibility, one can still see a clear trend about the types of structures selected vs the extent of reaction dilution. This is nicely shown, in looking at a histogram of the 3 concentration conditions and then the frequency of framework density value one obtains in the synthesis experiments. These are plotted across a range of **BEA*** to **MTW** in Figure 4. If we consider the extreme cases on the framework density axis, at low FD, there are almost no examples of a product formed at H$_2$O/SiO$_2$ = 14. Conversely for the highest FD products, almost all of them are occurring at this 14 value. The intermediate framework densities have a range of concentrations for product formation, and this is where the intermediate concentration value H$_2$O/SiO$_2$ = 7 makes a large contribution in terms of possible product types. This transitional range in concentration is also where we see the cases of more than one topology forming in a single synthesis, almost never with close values in

(41) Camblor, M. A.; Diaz-Cabanas, M. J.; Perez-Pariente, J.; Teat, S. J.; Clegg, W.; Shannon, I. J.; Lightfoot, P.; Wright, P. A.; Morris, R. E. *Angew. Chem., Int. Ed.* **1998**, *37*, 2122.
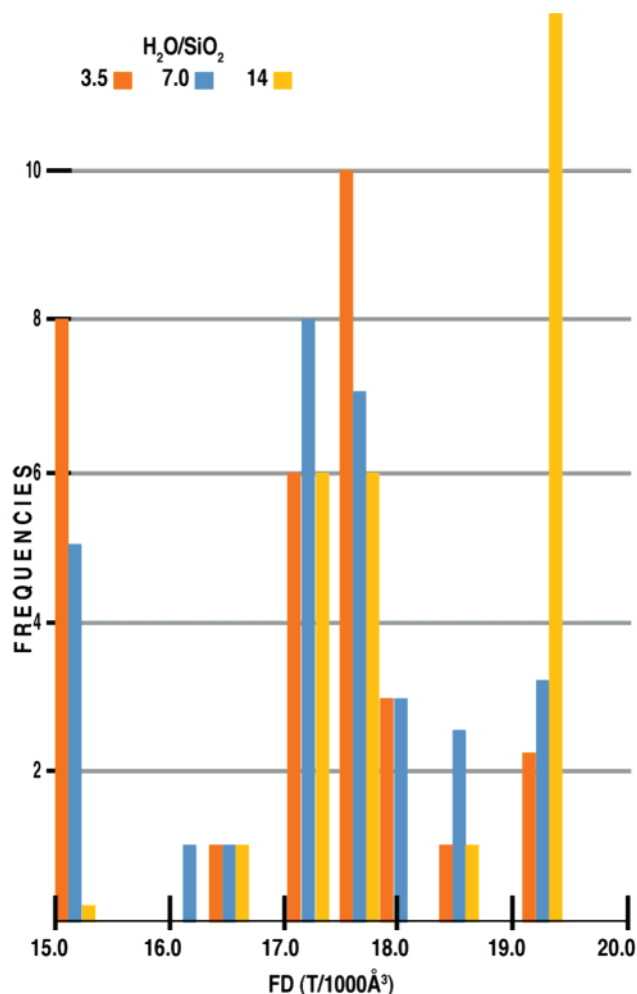
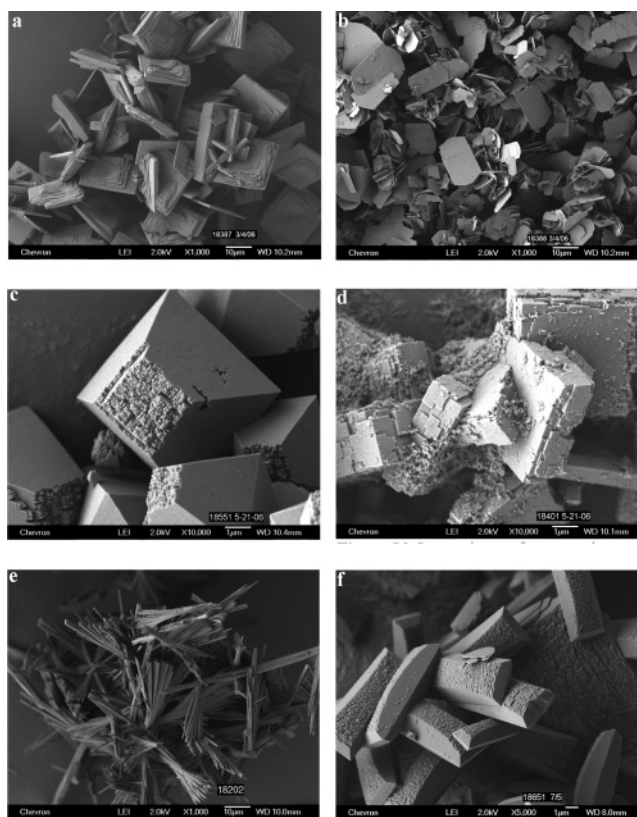**Figure 4.** Frequency of framework density types versus synthesis concentration.

Figure 5. (a) SEM of **STT** product made from G97 SDA. (b) Unknown layered material from G97. Is there a relationship between this phase and **STT**? (c) **BEA** zeolite made from G32. (d) Interesting surface growth features for **ISV** formation from G123. (e) **MTW** crystals from G24. (f) SEM image of **CON** crystallites made from G86.

framework density (i.e., **BEA***/**NES** in the case of G69 or **MFI**/**MTW** for G24).

We have alluded to the difficulty of generating a product when two factors come together. (1) The SDA is too large to successfully make a clathrate structure, and (2) the higher dilution experiment is favoring the formation of a high framework density product. Sometimes very large cage-based products will eventually form. In one interesting case, **ISV** was formed from a homopiperidine derivative (see Figure 2), G123. This SDA is the largest (C/N⁺ = 14) one used in our study. The product formation required 3 months at $H_2O/SiO_2 = 7$. There was still no product formation for the reaction at $H_2O/SiO_2 = 14$, out to 5 months. Here is a case where the SDA cannot make **MTW** so the ability to nucleate a viable host is very challenging. A similar situation using a very large SDA, previously described by us,[10] resulted in novel host SSZ-61 Fluoride is often seen preferentially bonded in such a way that it is contained within cage units[42] in silicate structures. If the best fit for the SDA is in a product with no cages (i.e., **MTW**), then the crystallization make take a very long time and is best aided by dilution if the impact of fluoride is to be minimized.

Effects on Crystallite Morphology. Because most of the earliest experiments using HF in zeolite synthesis used solvent

(42) Attfield, M. P.; Catlow, C. R. A.; Sokol, A. A. *Chem. Mater.* **2001**, *13*, 4708.

concentrations consistent with the known alkalinity syntheses at the time, most were run at H_2O/SiO_2 of 20−50. These are already more dilute than what we report in these studies. One would expect these earlier reactions to produce largely high framework density products, and that was indeed the case. Nice examples of large crystals (formed in slow reactions) were found for some clathrates and parallel one-dimensional pore system products. The large crystals sometimes produced better specimens for subsequent physical chemistry characterization. In a recent study we took advantage of the large crystals of **MTT** to do a single-crystal study that allowed us to locate the fluoride in the host product.[12] Figure 5 gives a survey of SEM micrographs, demonstrating the formation of large, well-formed crystals. Figure 6is a micrograph of a large crystal obtained in the reactions with G69.

Single-Crystal Opportunities: Details about Si−F Bonding. We initially could not identify the product for G69 from the powder diffraction pattern (Figure 7a). Single-crystal diffraction experiments showed that the larger crystals were an **STF** phase. Table S1 (Supporting Information) gives the crystallographic data for the structure solution of the guest/host product. The SDA adopts a certain configuration in the larger cage (which is bounded by two 10-rings), and the fluoride anions occupy the smaller cages surrounding the large one. This arrangement can be seen in Figure 8. Interestingly, the as-made **STF** phase prepared with G69 possesses a triclinic symmetry of P$\bar{1}$. This is different from a previously reported[43] monoclinic symmetry of **STF** products from fluoride-mediated syntheses with a different SDA molecule, but it is also higher than the
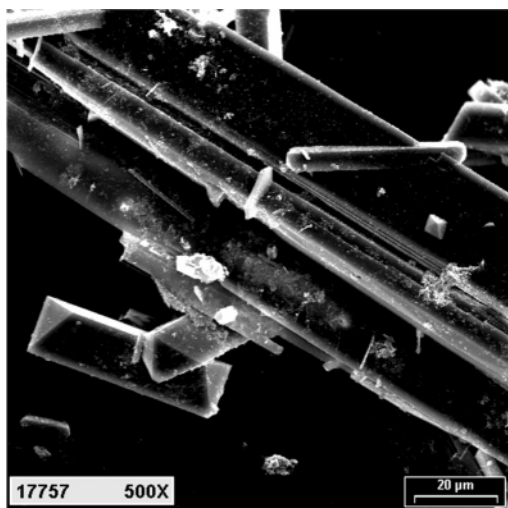
Figure 6. Unusually large crystals from a synthesis run using G69. Single-crystal work was carried out to determine both the host structure and orientation of the guest molecule.
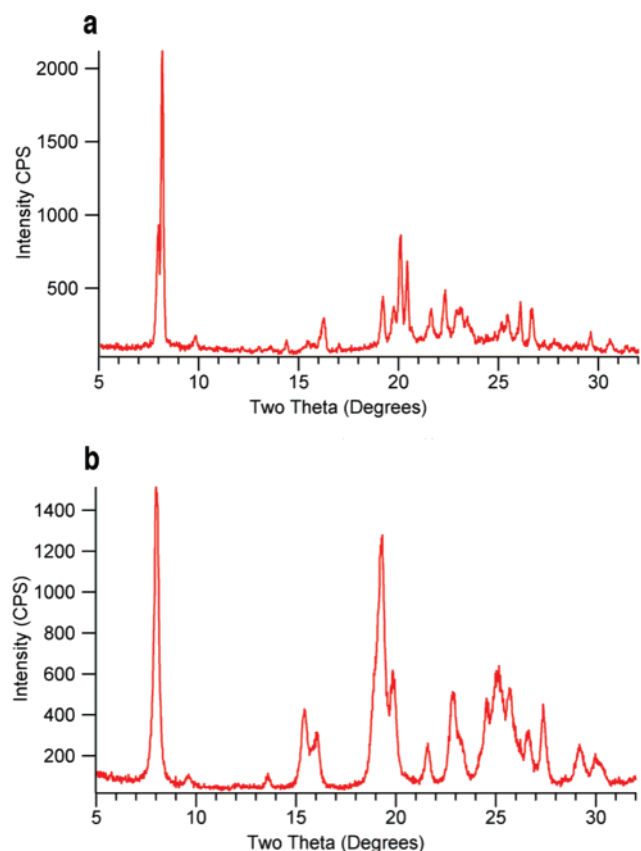

Figure 7. (a) X-ray diffraction pattern for the product from G69 at 170 °C and $H_2O/Si = 7$. The sample contains not only very large crystals of **STF** but smaller ones from **CON.** (b) Typical X-ray diffraction pattern for SSZ-35 (**STF**).

$P1$ symmetry found by Patarin and co-workers.[44] Subsequent analysis of the remaining diffraction peaks in the powder diffraction pattern revealed a minor impurity phase to be a **CON** intergrowth product. Note that **CON** is prepared with G69 at the highest gel concentration at 170 °C. Figure 7b shows a

(43) Fyfe, C. A.; Brouwer, D. H.; Lewis, A. R.; Villaescusa, L. A.; Morris, R. E. *J. Am. Chem. Soc.* **2002**, *124*, 7770−7778.
(44) Harbuzaru, B.; Roux, M.; Paillaud, J. L.; Porcher, F.; Marichal, C.; Chezeau, J. M.; Patarin, J. *Chem. Lett.* **2002**, 616−617.
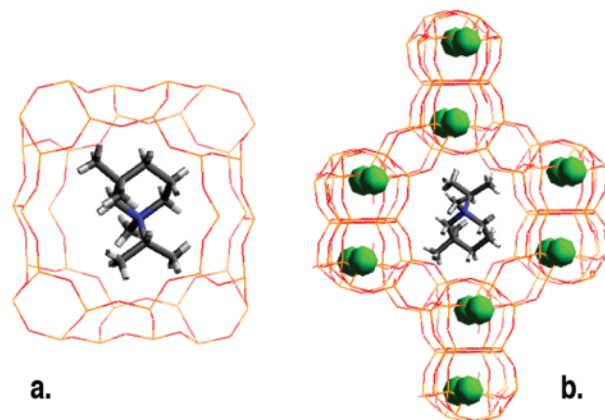
Figure 8. Images of the single-crystal structure of G69 in **STF**: (a) SDA surrounded by only the large cage; (b) small cages along with the symmetry-related positions of the fluoride ions.

typical pattern for **STF**, and it is clear that there could be some confusion between the two patterns. The single-crystal work shows there is a particular configuration of the SDA, G69, within the **STF** cages, as well as an ordered array of fluoride anions in which a percentage of the small cage sites are occupied. These details can be seen in Figure 8a,b.

There are 7 Si atoms in the asymmetric unit, and the single-crystal work shows that fluoride interacts with one center giving a measured distance of 1.900(6) Å. This is an unusually long Si−F distance, which has been observed also in a nonzeolitic system with F^- bridging two Si centers.[45] However, in the zeolite **STF**, made with G69, the F is not bridging. Furthermore, the F atoms occupy an axial position of a trigonal bipyramidal unit (we will say more below about the occupancy issue). The trans-oxygen atom has a long Si−O bond of 1.656(3) Å, which may reflect some of the distortion introduced locally. The equatorial Si−O distances are normal. All other Si centers are tetrahedral and have the expected Si−O bond distances near 1.6 Å. Thus, the presence of the fluoride has introduced considerable strain in the local environment where it sits in a pseudocage environment.

In studies of zeolite materials there have been some other examples where the refined Si−F distances have exceeded 1.8 Å. Zeolites **CHA**, **SAS**, and **AFS** are examples of all-silica frameworks containing these longer Si−F bond lengths from single-crystal data. However, in some instances there has been follow-up using NMR to assess what the bond distances should be. In a work on the AFS material made from fluoride use, Morris and co-workers point out that both the SDA and the local F^- anion contribute in interacting with the Si tetrahedral.[46] In that work it was shown that nearest-neighbor oxygens (with reference to the Si center bonded to F) experience some distortion as well. In a number of single-crystal studies on Si−F bonding in zeolite materials, there has been some discussion that the true local structure can be masked by the averaging of [SiO_{4/2}F^−] units with the fluoride present and absent. Incomplete occupancy of fluoride anions in the structure and the potential for dynamic disorder has led to the reporting of Si−F bond distances ranging from 1.84 to 1.99 Å. In the case of the same

(45) Tamao, K.; Hayashi, T.; Ito, Y.; Shiro, M. *Organometallics* **1992**, *11*, 2099.
(46) Burton, A. W.; Darton R. J.; Davis M. E.; Morris, R. E.; Ogino, I.; Zones, S. I. *J. Phys. Chem. B* **2006**, *110*, 5273−78.

Table 4. Comparison of Products under HF, OH⁻ Reaction Conditions[a]

no.	C/N⁺	HF products	all SiO₂	OH⁻ products SAR	OH⁻ products SBR
G11	7	AST, NON	NON	NON	
G74	8	AST, DDR		DDR, MFI	SGT
G210	8	NON, NON, Amo/NON			
G200	8	NON			
G24	9	MEL, MTW, MFI	MTW	AEI	SSZ-36
G80	9	BEA, DDR, DOH, SGT		CHA, MFI, MTW	SSZ-36
G65	9	MFI, DOH	SSZ-31	AEI, MFI	SSZ-36
G212	9	BEA*, NON			
G25	9	NON	MTW, NON	MTW, NON, CHA	
G49	10	MEL/MFI	MEL	MTW	MEL
G39	10	STF		AEI, STF	STF
G55	10	NON	NON	MFI	SSZ-36
G61	10	MFI, STF	SSZ-31	CHA, MFI	MEL
G213	10	BEA		ERS-10, MTW	
G40	11	SFF	SFF	SFF, AEI	SFF
G71	11	MFI	MFI	MFI, CHA	MFI
G51	11	STF, NES, CON	SSZ-31	CHA	SSZ-36
G50	11	MEL	MEL	CHA, MEL	MEL
G69	11	BEA, NES, CON, STF		CHA	
G77	11	BEA*, STF	SSZ-31	AEI, MWW, STF	STF
G81	11	BEA*	SSZ-31	CHA	
G52	12	MEL		unknown, MEL	
G73	12	MEL		CHA, MEL	SSZ-31
G122	12	ITE		AEI	
G93	13	EUO		EUO	EUO
G105	13		SSZ-43	SSZ-43	SSZ-43
G121	13	BEA*			
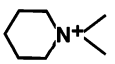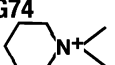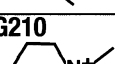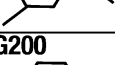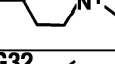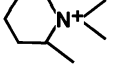
[a] SAR = SiO₂/Al₂O₃ and SBR = SiO₂/B₂O₃.

Table 5. Energy-Minimized Calculations for SDA/Hosts Where C/N⁺ ≤ 9[a]

SDA	AST 10	NON 22	SGT 16	DDR 20	DOH 34	STF 16	ITE 16
G11	-13.1	-6.2	-8.4	-6.3	-3.9		
G74	-14.1	-5.9	-9.2	-7.2	-4.4		
G210	-11.4	-7.0	-9.6	-7.1			
G200	-5.5	-6.9	-7.1	-7.2			
G32	-10.0	-3.5*	-10.3*	-8.0		-9.5*	-8.7*
G25		-6.8*	-9.9	-8.1		-9.3*	-8.9*

[a] The asterisks indicate calculated entries determined in ref 14 (Burton et al.). The number given right under the structure codes (i.e., 22 in the case of NON) indicates the number of T atoms in the cage where the SDA resides. There are no results for MFI and MEL.

zeolite under discussion here, but made with a different SDA, Morris et al. had contrasted the longer Si–F distances with those obtained by NMR where a value of 1.74 Å was found.[47] The latter agree well with density functional theory simulations for fluoride ions in SOD and FER zeolite frameworks where the site of the Si–F interaction causes a trigonal bipyramidal coordination with distances from 1.76 to 1.71 Å. So these methods suggest a shorter bond distance than seen by crystallography (where incomplete occupancy and distortion can have an impact).

Comparison of Product Selectivities for the HF System vs OH⁻ for Zeolite Synthesis. We have summarized most of our results in the HF/SIO₂ system in Table 4, where we also show the types of framework selectivities observed when the same SDA had been used in the OH⁻ media reactions. These studies had been described previously by Nakagawa and co-workers.[24] Besides seeing that the product selectivities may sometimes be different in these comparisons, there is also the interesting feature that certain structures appear relatively frequently in the OH⁻ systems and do not appear in the HF study, here with the same piperidine derivatives. A frequent product for the more Al-rich syntheses in OH⁻ media is either SSZ-39 (**AEI**) or SSZ-13 (**CHA**). If we look at our data, neither open framework product is observed in the HF/SiO₂ reactions.

While **AEI** has not yet been observed in any HF/SiO₂ chemistry to our knowledge, the strongly selective SDA *N,N,N*-trimethyl-1-adamantammonium can specify the **CHA** structure.[9] In the Camblor study, the same SDA can make either **STT** or SSZ-31[48] (a faulted, polymorphic 12-ring not yet assigned a structure code) as the reaction becomes more dilute. A number of large piperidine derivatives in this study make SSZ-31 in the OH⁻ media under all-silica conditions. However, it is not observed here under the HF conditions.

In one instance, we see that there is no overlap of products. G80 yields phases like **SGT** and **DDR** not seen under the OH⁻ conditions. This is interesting because our calculations (see next section) would indicate that these should be favorable guest/host products. But the inorganic chemistry in the alkaline media (with alkali metal cations present as well) does not promote these structures.

We have already discussed some issues surrounding the **ITE** formation and the polymethylated ring derivatives. Only one experiment produces **ITE** here, but in the OH⁻ media, especially with boron present, a number of SDA produce what we have described as SSZ-36.[34] SSZ-36 defines a range of intergrowth structures with varying proportions of **ITE** and **RTH** faulting probabilities. The contrast of the products observed in these two different reaction media for the same SDA, once again, points up the importance of kinetic control in the assembly of these guest/host products.

Energy Minimizations/Molecular Modeling of Piperidine Derivatives in Selected Zeolites. Since we have a large database of products formed, are the results consistent with energetic predictions? In this section we look at the extent of favorable packing of guest molecules into the hosts observed. As we

(47) Fyfe, C. A.; Brouwer, D. H.; Lewis, A. R.; Villaescusa, L. A.; Morris, R. E. *J. Am. Chem. Soc.* **2002**, *124*, 7770.

(48) Lobo, R. F.; Tsapatsis, M.; Freyhardt, C. C.; Chan, I. Y.; Chen, C. Y.; Zones, S. I.; Davis, M. E. *J. Am. Chem. Soc.* **1997**, *119*, 3732.
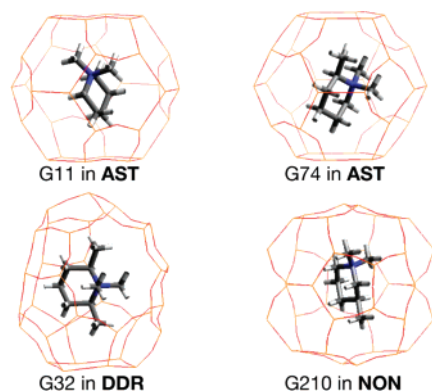
Figure 9. Representations of closely related SDA in the clathrate host products **AST**, **DDR**, and **NON**.

pointed out in the Experimental Section, van der Waals interactions will dominate the calculations. We will want to see if there are critical differences in energy that define the expected product selectivity. Sometimes we will see that there are not critical differences calculated yet selectivity is seen. This implies that other factors than the SDA are more important in determining product selectivity.

Table 5 shows the calculated energy minima for the smaller molecules examined in our syntheses. The energies are reported on a per T atom basis. The energy/SDA molecule can be determined by multiplying the per-T-atom stabilization by the number of T atoms/cage (or intersection) shown below the three-letter IZA code in the table. The molecules in Table 5 have two methyl substituents at the nitrogen position and either one or two methyl groups at other positions within the piperidine ring.

An interesting trend immediately appears for these small molecules. Large stabilization energies are generally calculated for the **AST** framework because it is able to accommodate a relatively large number of small SDA molecules in the overall structure (10 T atoms/cage) compared to other competing phases like **NON** (22 T atoms/cage) or **DDR** (20 T atoms/cage). The simplest molecule, G11, produces **AST** and **NON** phases in the fluoride-mediated syntheses. G11 possesses a calculated stabilization of −13.1 and −6.2 kJ/mol T atom in **AST** and **NON**, respectively. **AST** appears only in the more concentrated fluoride gels, and it has not been reported to crystallize in all-silica gels in the absence of fluoride. Although D4R units generally increase the energies of all-silica structures, the ability of fluoride to promote or stabilize all-silica D4R cages has been well documented in the literature. This is consistent with our observation that **AST** is replaced with other phases as the fluoride concentration is decreased.

When a methyl group is added at the 2-position of the piperidine ring, the stabilization energy is further increased in the **AST** structure. Here we can see that the stabilizations provided by both the SDA and the fluoride ion promote the formation of the **AST** structure. However, G210 (−11.4) and especially G200 (−5.5) illustrate that the placement of the methyl group can significantly alter the shape of the molecule to the extent that it no longer has a favorable fit in the **AST** cage. In these cases, the stabilization energy calculated for the **AST** framework is not sufficient to compensate for the differences in framework energy with **NON**. Some of these SDA relationships in the clathrate products are shown in Figure 9.

Table 6. Energy-Minimized Calculations for SDA with C/N+ of 9 or Greater and Single Heterocycle Rings[a]

SDA	NON 22	SGT 16	DDR 20	DOH 34	MFI 24	MEL 24	STF 16	ITE 16	STT 16
G80	-5.0	-10.0	-7.8	-4.6	-5.7	-5.8	-9.7*	-8.7*	
G65	-4.9	-9.7	-7.7	-4.6	-5.6	-5.6	-9.3*	-8.8*	
G39	+0.6	-10.4	-7.9		-4.8	-4.8	-10.4*	-9.9*	
G55	-6.0‡	-10.5	-8.2		-5.4	-6.0	-10.4*	-9.3*	
G61		-4.8	-6.0		-6.4	-5.8	-10.2	-9.1	
G77		-9.5*			-3.8	-5.0	-11.2*	-10.4	-10.4
G50				cis	-5.0	-5.4	-6.8*	-9.6*	
				trans	-5.2	-5.7	-10.2*	-10.6*	
G71				cis	-5.7	-4.8			
				trans					
G40				cis	-5.5	-5.8	-10.9*	-10.9*	
				trans					
G49				cis	-6.2	-6.3	-9.2		
				trans	-5.9	-6.1	-9.8		
G48				cis	-3.7	-5.8	-8.5	-10.2	
				trans	-4.8	-5.5	-9.9	-10.5	

[a] The asterisks indicate calculated entries determined in ref 14 (Burton et al.). The number given right under the structure codes indicates the number of T atoms in the cage where the SDA resides.

In our previous modeling studies of piperidine derivatives, we noted that molecules that give calculated stabilizations less than −6.0 kJ/mol of T atom in **NON** are generally successful in producing nonasil phases. In Tables 5 and 6 we see that the energies for G11, G210, G200, and G55 fall within this range. As we previously observed for the **AST** case, the placements of the ring substituents have dramatic effects on the calculated energies for the piperidine derivatives within the **NON** cage. SDA that are too large or do not possess the proper shape (G32, G80, G65, G39) do not yield a **NON** phase. When the energy is not favorable for **NON**, we begin to see phases like **DDR** (and **SGT** in one case). On the basis of correlations of measured and calculated framework energies with framework density, we expect the empty **NON** framework to be more stable than **DDR**. Therefore, it is not surprising that greater stabilization is required in the **DDR** framework compared to **NON**. For example, we see that G11, G210, and G200 give similar stabilization energies, yet **NON** is the preferred phase. G32 is interesting because, in hydroxide-mediated syntheses, we do not observe **DDR** as a

Table 7. Energy-Minimized Calculations for Spiro Piperidine Derivatives and Molecules with C/N⁺ = 11 and Larger[a]

SDA	SGT 16	DOH 34	MFI 24	MEL 24	STF 16	ITE 16	STT 16	EUO 28	NES
G93 CH₃					NO FIT	NO FIT	-5.9	-5.6	
G122	-4.5				-8.2	-11.8	-8.7		
G73 cis		cis	-3.3	-6.0	-7.7	9.2	-10.3		
G73 trans		trans	-3.8	-5.3	-7.4	-10.3	-10.8		
G97					-10.9	-11.3	-11.8		
G69			-4.0		-10.6	-10.4	-11.1		
G51			-4.0	-5.2	-10.3	-10.4			-9.1
G81				-5.9	-10.2				

[a] The number given right under the structure codes indicates the number of T atoms in the cage where the SDA resides. There are no results for AST, NON, and DDR.

G122 in ITE

Figure 10. Representation of the hexamethylated homopiperidine ring (G122) and its fit into the cage of **ITE**.

phase yet we do in the fluoride-mediated syntheses. As the energy differences become greater, we encounter a transition period. G74, for example, has a calculated difference of −1.3 kJ/mol in favor of **DDR**, and the molecule does indeed produce **DDR**. G25, on the other hand, possesses the same difference, yet it is very selective for Nonasil in both fluoride- and hydroxide-mediated syntheses. G32 and G80 possess over-whelmingly better energies in the **DDR** framework. Another interesting observation is that G80 crystallizes **SGT**, **DDR**, and **DOH**. None of these phases are observed in the hydroxide chemistry! In our previous work, we noted that **SGT** does not appear to be as kinetically favored as many other cage-based zeolite structures. While it often has excellent calculated fits (< −9.5 kJ/mol T atom) for molecules like G210, G32, G39, G55, and G25, **SGT** rarely crystallizes when the calculated energies are as good as those determined for phases like **STF** which have lower framework densities. However, we do observe that G80 succeeds as an SDA for this phase.

One result that cannot easily be rationalized from the molecular modeling is the selectivity of molecules G65 and G80 for **DOH**. The **DOH** structure has one large cage that is surrounded by several cages that are too small to accommodate the SDA molecules. Therefore, there can be only one SDA molecule/34 T atoms in this structure, and hence, the stabilization on a per T atom basis will be small even when the absolute energy/SDA molecule is quite favorable. Although the density of the **DOH** framework structure suggests its framework (with no occluded SDA molecules) is energetically favored compared to most other competing phases, from a purely thermodynamic standpoint it is difficult to explain how this phase forms when the SDA offers so little stabilization (−4.6 kJ/mol T atom) to the framework.

In Tables 6 and 7 we observe some other noteworthy trends. In the HF chemistry, **STF** (**SFF** for G40) is clearly favored over **ITE** when the calculated energies are calculated to be close

to or in favor of **STF** (see G39, G61, G69, and G77). Only in the case of G122, where there is −3.6 kJ/mol T atom difference that favors **ITE**, do we see that **ITE** is preferred over **STF**. Figure 10 shows the relationship of the space-filling of G122 in **ITE**. This is different from what we observed in borosilicate chemistry in hydroxide media. In those cases, we saw that molecule G25, G24, etc., gave SSZ-36 (**ITE/RTH** intergrowths) although **STF** had a better calculated fit than **ITE**. In the HF chemistry, for these same molecules we do not observe either of these phases. This may reflect that the kinetic routes to successful nucleation follow different paths for silicate organization.

As long as denser phases are not preferred, **STF** phases are generally observed when the stabilization exceeds −10.2 kJ/mol of T atom. For example, G39 (which is very specific for **STF**) and G55 (specific for **NON**) both possess stabilizations of −10.4 kJ/mol of T atom in **STF**. However, G39 (+0.6) does not have a favorable fit in **NON,** while G55 does (−6.0). As we have previously discussed, in correlating phase selectivity with stabilization, it is not sufficient to know that a molecule has a "good fit" within a given structure. One must also know how well the molecule fits in potential competing phases. Early in our studies with the piperidine molecules, it seemed difficult to explain why some molecules were specific for **MFI** or **MEL** phases while similar molecules were specific for **STF** or **SFF**. We now observe that **MFI** and **MEL** phases form when the calculated stabilizations exceed −5.5 kJ/mol of T atom (G49, 52, 50, 65, 80, and 73). In general, when the calculated stabilization is at least −4.5 kJ/mol of T atom in favor of **STF** over **MFI** or **MEL** (G39, 40, 77), **STF** is the preferred phase. Only G61, which is −3.8 kJ/mol of T atom in favor of **STF**, is the exception; in this case, both **STF** and **MFI** are formed. Figure 11 demonstrates these relationships graphically for the relative stabilization of **STF** over **MFI** or **MEL**. The y-axis shows how much more stable a given molecule is calculated to be in **STF** (or **SFF**) compared to the **MFI** or **MEL** framework (on a per SiO₂ basis). The pentasil framework chosen as the basis of comparison is the one with the better calculated fit for a particular molecule. For differences in calculated stabilization below about 4.5 kJ/mol, the pentasil phases seem to be favored while **STF** is observed when the magnitude of its stabilization is 4.5 kJ/mol greater than for the pentasil frameworks.

Another interesting topic is the phase selectivity of **MFI** versus **MEL**. These two zeolites have similar framework structures with two-dimensional systems of channels. The crystal structures of the two zeolites differ by a single symmetry operation. Mirror planes relate the layers in MEL, while the same layers in **MFI** are related by inversion centers. The different symmetry operations yield channel intersections of different shape and dimensions in the respective zeolite frameworks. Von Koningsveld and co-workers have performed an
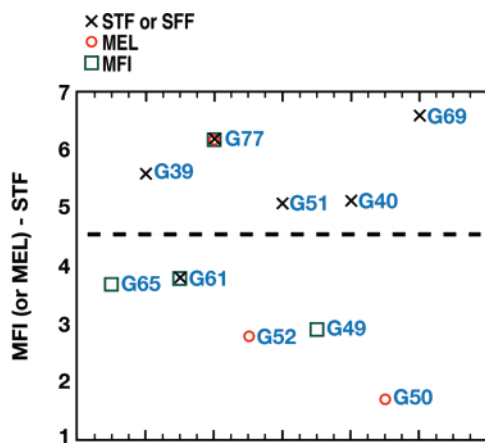
Figure 11. Differences in calculated stabilization (kJ/mol of T atom) for different piperidine derivatives in pentasil zeolites (**MFI** or **MEL**) versus those determined in **STF** (or **SFF** in one case). The *y*-axis indicates how much greater the silica is stabilized in **STF** (or **SFF**) rather than in **MFI** (or **MEL**). If **MEL** possesses a greater stabilization than **MFI**, then **MEL** is chosen as the basis of comparison with **STF**. The cross hatches indicate molecules that make **STF** or **SFF**, the circles indicate phases that make **MEL**, and the squares indicate molecules that make **MFI**.

insightful molecular modeling study that explains the selectivity of molecule G50 for **MEL**.[33] They examined the fits of both the cis and trans isomers of G50 in the **MFI** and **MEL** frameworks. An important observation from that study was that **MEL** possesses two different kinds of channel intersections while **MFI** possesses only one. For **MEL**, both channel intersections must be considered to make sound comparisons. A potential complication in making comparisons of the 3,5-dimethylpiperidinium derivatives is that we do not know the relative ratios of each isomer that are incorporated into the zeolite structure or whether only a single isomer is occluded. We do know that the parent amine is about 75/25 cis/trans. We therefore might expect the synthesis behavior to be dominated by the cis compound, but we cannot know this with absolute conviction. In the von Koningsveld work, all combinations of isomer/intersection pairs were calculated and the lowest energy pairs were used in making comparisons between the **MEL** and **MFI**. Note that the energies we report in Table 7 are for the cases where either the cis occupies both intersections or the trans occupies both intersections.

For the cases where either of the two phases forms, **MFI** always crystallizes when it is predicted to have the better fit or when the two frameworks have very similar framework energies. From an energetic standpoint, this is consistent with the fact that the **MEL** framework has a higher energy than the **MFI** framework. **MEL** forms when its stabilization is at least −0.4 kJ/mol in its favor. G49 presents an interesting case in which an **MEL**/**MFI** intergrowth is formed. Here the cis and trans isomers are favored in **MEL** only by −0.1 and −0.2 kJ/mol of T atom, respectively.

Before we started this work, it was difficult to rationalize why molecule G71 was so selective for **MFI** although G50 was remarkably selective for **MEL**. In G71 an etheric oxygen atom has replaced the methylene unit at the 4 position in the piperidine ring. Some of our initial speculations involved hydration effects around the oxygen atom that might influence the ability of one phase to form over the other. Conventional wisdom might dictate that these molecules should have the same phase selectivity because their shapes are so similar. However, in Table 7 we
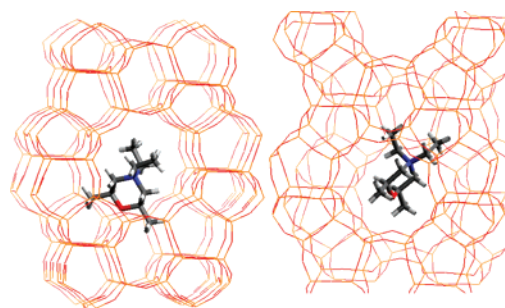

Figure 12. Images of the energy-optimized position of the cis isomer of G71 in **MFI** with views (left) along the straight 10-ring channel and (right) along the sinusoidal 10-ring channel.
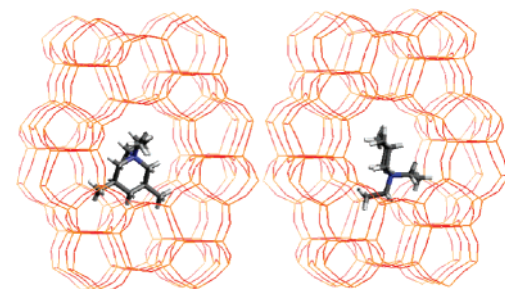

Figure 13. Images of energy-optimized configuration of (a) cis isomer of G50 in **MFI** with view along the straight 10-ring channel for initial position similar to that found for the minimum configuration of G71 (−4.6 kJ/mol of T atom) and (b) the actual minimum energy (configuration of *cis*-G50 (−5.0 kJ/mol of T atom) in **MFI**.

see that the cis derivative of G71 has a stabilization of −5.7 kJ/mol T atom in **MFI** while G50 is only −5.0 kJ/mol T atom. In **MEL**, just the opposite is observed. Figure 12 shows the energy-optimized configuration of the cis isomer of molecule G71 in **MFI**. In this configuration, each methyl group points into a separate window located at the **MFI** channel intersection. The etheric oxygen atom is positioned 2.6 and 2.8 Å above a pair of framework oxygen atoms. This is a suitable van der Waals contact distance. However, when the G50 molecule is placed in the same initial position for a docking calculation, the steric repulsions between the methylene protons and the framework oxygen atoms force the molecule away from this position (see Figure 13) to give a configuration that does not allow van der Waals contacts that are as ideal for those with G71; in fact, an entirely different configuration (Figure 13b) was found to have the minimal energy in the **MFI** structure. The explanation is unexpected but remarkably simple. In this case, the steric effects of a single pair of methylene protons have a significant effect on the stabilization of the SDA molecule.

Conclusions

The combination of synthesis parameters for making guest/host complexes from chemistry with silicate, fluoride anions, and a series of piperidine-based quaternary ammonium compounds (SDA's) has shown some clear trends in product selectivity but exceptions follow as well. This is not unexpected in a reaction system that has increasingly been described as having steps with small energy changes. Some very detailed and challenging calorimetry experiments carried out by the groups of Davis and Navrotsky over several years helped to demonstrate this.[49] The generalizations we observe are a

tendency for more open-framework products under concentrated reaction conditions with suitably large SDA. This is consistent with the initial report of this behavior by Camblor in using adamantyl derivatives. We rarely make open framework products when conditions become more dilute. This may serve to answer the question why historically a new phase had not been discovered in the initial uses of this reaction system. Instead the reporting of large crystal products for high framework density products (clathrate and 1D hosts like **MTW**, **MTT**, **TON**, and ZSM-48) seemed the norm. We do find that smaller SDA will make clathrates, even under highly concentrated conditions, unless a particular guest/host interaction offers itself as an intervention. Our unexpected results for G32 are an example.

Molecular modeling allowed us to interpret many of the product selectivities on the basis of favorable energetics for the guest "fit" in the product cages. Some subtleties emerged such as differences in space-filling of methylene protons (rather than a change in hydration) in G71 being responsible for the change in product selectivity when an isostructural morpholine SDA was used in contrast to the piperidine SDA. In some instances only certain conformations could successfully nucleate a host lattice. In extremes this may be a very slow process as was seen for the G123 directed synthesis of our lone **ISV** product.

(49) Piccione, P. M.; Yang, S.; Navrotsky, A.; Davis, M. E. *J. Phys. Chem. B* **2002**, *106*, 3629−38.
(50) Burton, A. W. In *Introduction to Zeolite Science and Practice*; van Bekkum, H., Cejka, J., Corma, A., Schuth, F., Eds.; Studies in Surface Science and Catalysis Series; in press, 2007.

When the syntheses are carried out in all-silica reactions in hydroxide media, there is still the issue of what contribution the requisite framework defect provides. Burton has addressed this to some degree in a recent discussion.[50] In addition it would be interesting to determine why there is great product selectivity for cage structures like **AEI** and **CHA** in hydroxide runs (and **ITE** when boron is present), but these factors do not carry over to the silicate chemistry in the presence of HF. We do not have a suitable modeling approach to explain this as yet.

Supporting Information Available: Appendix 1, showing a number of the structure representations for the 17 product topologies given in Table 2, Appendix 2, giving the SDA synthesis examples which characterize the variations used in making all of the SDA in Table 2, Table S1, giving the crystallographic data for the structure solution of the guest/host product, and mn1752.cif, providing the atomic coordinates and anisotropic thermal factors (file can be read by most crystal viewing programs). This material is available free of charge via the Internet at http://pubs.acs.org.

JA0709122